# Tropical Subsurface Salinity and Tritium Distributions in the Pacific: Their Differences and Formation Mechanisms*

MASAMI NONAKA

*International Pacific Research Center, School of Ocean and Earth Science and Technology, University of Hawaii, and Frontier Research System for Global Change, Tokyo, Japan*

KENSUKE TAKEUCHI

*Institute of Low Temperature Science, Hokkaido University, Sapporo, Japan*

15 December 1999 and 24 November 2000

ABSTRACT

While high salinity water extends to the equator in the upper thermocline of the Pacific in the Southern Hemisphere (SH), it hits the western boundary (WB) farther north of the equator in the Northern Hemisphere (NH), suggesting that no interior pathway exists to the equatorial region. By contrast, high tritium water appears on the equator in the central Pacific, apparently through a NH interior pathway within the thermocline. The mechanisms of forming these salinity and tritium distributions and the causes of their difference are investigated using a realistic ocean general circulation model (OGCM).

The OGCM reproduces the properties of tropical salinity distribution quite well and displays interior pathways in the NH. Analysis indicates that the observed salinity distribution is compatible with the existence of a NH interior pathway. Key to the hemispheric difference in thermocline salinity is the sea surface salinity (SSS) distribution in relation to the so-called WB (interior) exchange window, from which subducted water goes to the equatorial region through the WB region (interior ocean). In the NH, high SSSs are found only in the WB exchange window, and high salinity water thus appears to turn onto the WB before reaching the equator. In the SH, on the other hand, high SSSs are found in both the WB and interior exchange windows, and, as a result, high salinity water extends to the equatorial region through both the WB region and interior ocean.

The sea surface tritium field has high values near the eastern boundary within the interior exchange window in the midlatitude North Pacific. Thus, high tritium water takes the NH interior pathway to the equatorial region after the subduction. This is demonstrated by a passive tracer experiment with a sea surface distribution resembling that of tritium. This result suggests that the apparent differences between the isopycnal salinity and tritium distributions are largely due to differences in surface distribution, raising caution about interpreting ocean circulation with tracer fields alone.

## 1. Introduction

In a meridional salinity section in the central Pacific (Fig. 1a), a high salinity tongue extends from the subtropics to the Tropics on either side of the equator. Figure 2a depicts the tropical salinity distribution on the $\sigma_\theta = 24.5$ isopycnal surface, a density surface around which high salinity cores are located on both hemispheres. In the Southern Hemisphere, a high salinity tongue (>35.0 psu) extends northwestward all the way to the western boundary and the equator, and a strong salinity front forms in the equatorial region. In the Northern Hemisphere, on the other hand, high salinity water extends southwestward from the outcrop line toward the western boundary, but does not extend to the equatorial region. To the south of the high salinity water, a band of relatively low salinity exists around 10°N.

In an isopycnal surface analysis, Tsuchiya (1968) showed that these high salinity tongues in the Northern and Southern Hemispheres and the low salinity band extend in the direction of the geostrophic flow. As shown in Fig. 2a, the high-salinity tongues emerge from the outcrop lines of the isopycnal surface in the subtropics, suggesting that subtropical sea surface high salinity water is transported to the Tropics. Consistent with this, the temporal change of the area of the high salinity water that appears in the 137°E section correlates with the change of the wind stress curl in the subtropical North Pacific with a time lag of 0–2 yr (Shuto 1996).

The ocean circulation that transports high salinity wa-

* School of Ocean and Earth Science Technology Contribution Number 5329 and IPRC Contribution Number 74.

*Corresponding author address:* Dr. Masami Nonaka, IPRC, SOEST, University of Hawaii, 1000 Pope Road, Honolulu, HI 96822. E-mail: nona@soest.hawaii.edu

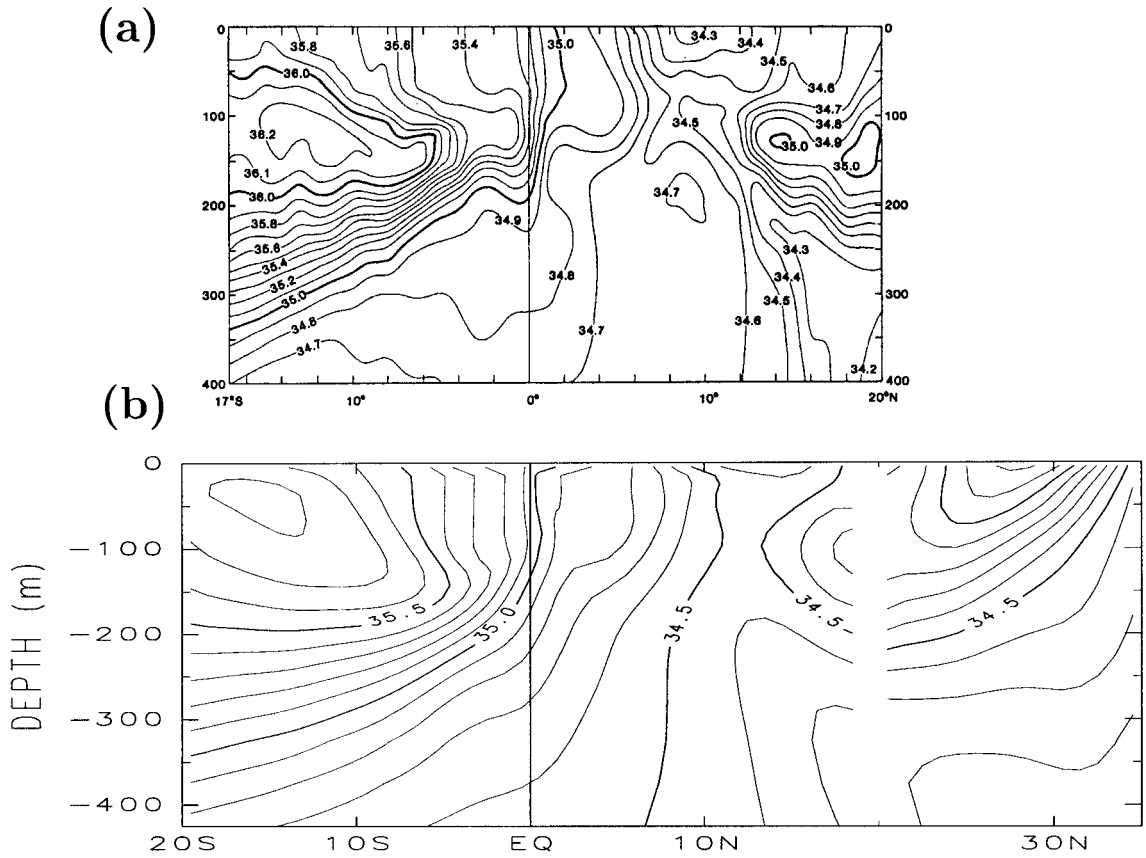


FIG. 1. (a) Mean distributions of salinity between Hawaii and Tahiti near 155°W (after Wyrtki and Kilonsky 1984). (b) Meridional section of annual mean salinity field of the model result at 155.5°W. Contour intervals are 0.1 psu.

ter from the subtropics to the tropical thermocline (Figs. 2b,c), has been studied recently (McCreary and Lu 1994; Liu 1994). This wind-driven circulation is asymmetric about the equator, owing to the northward displacement of the annual-mean atmospheric Intertropical convergence zone (ITCZ) in the Pacific (Xie 1996, and references therein). In particular, the downward Ekman pumping weakens just north of the equator around 10°N, where a band of high potential vorticity forms the so-called ''potential vorticity barrier'' (Lu and McCreary 1995). This weak Ekman downwelling tends to prevent the water parcels from entering the equatorial region through the interior ocean and to force them to go westward. It thus appears plausible that this asymmetry of the flow pattern can explain the hemispheric asymmetry of the observed isopycnal salinity distribution.

The existence of an interior pathway along the thermocline to the equator in the Northern Hemisphere is, however, suggested by the observed subsurface tritium distribution. A high tritium tongue appears to extend into the central equatorial Pacific from the North Pacific (Fine et al. 1981, 1987; Fig. 3a). As shown by the zonal-$\sigma_\theta$ section along the World Ocean Circulation Experiment P04 line at 10°N (Fig. 3b), this high-tritium penetration, illustrated by zonal maxima in the central Pacific, takes place on a range of isopycnal surfaces in the upper thermocline. Recent detailed analysis of tropical potential vorticity supports the possibility that an interior flow may pass the potential vorticity barrier underneath the ITCZ (Johnson and McPhaden 1999). A number of ocean general circulation models (OGCM: Nonaka 1994; Gu and Philander 1997; Rothstein et al. 1998) and intermediate models (Lu et al. 1998; Liu and Huang 1998) under observed wind forcing also show an interior pathway from the subtropics to the equator in the North Pacific, while the flow pattern still has strong asymmetries about the equator due to the weakened Ekman downwelling around 10°N.

Both observed tritium distributions and recent modeling studies suggest the existence of the interior route from the North Pacific to the equatorial region. But on the other hand, the high salinity tongue reaches the equator only through the western boundary region in the Northern Hemisphere, making it appear to be inconsistent with the notion that there exists a northern interior water pathway. To address this contradiction, we pose the following questions: Can we conclude from the northern salinity distribution that there is no interior pathway in the Northern Hemisphere? Why is its dis-

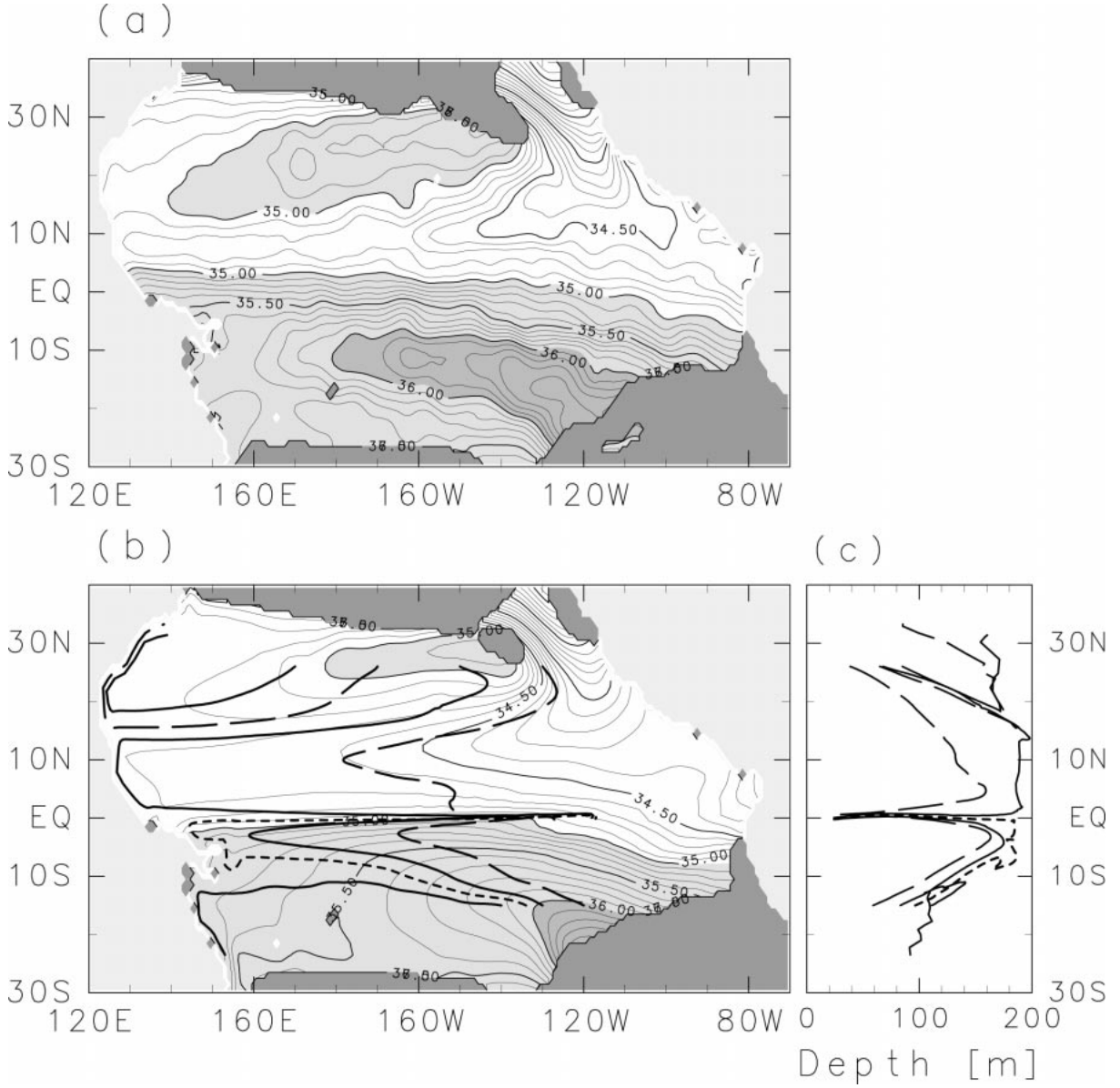


FIG. 2. Annual mean (a) climatology and (b) model result of salinity on the $\sigma_\theta = 24.5$ surface. Trajectories (thick lines) of water parcels starting at 15°S, 26°N, on the isopycnal surface $\sigma_\theta = 24.5$ are superimposed on (b). Contour intervals are 0.1 psu. Lighter (darker) shading shows salinity higher than 35.0 (36.0) psu. Darkest shaded regions show outcropping area. (c) Trajectories same as shown in (b) but projected on latitude–depth section.

tribution different from that of the tritium distribution, given that they are advected by the same flow?

This paper is organized as follows. In section 2, the model and the resultant salinity field are introduced. The mechanism of forming the salinity field and whether it is consistent with the existence of an interior pathway is examined in section 3. In section 4, the differences between the salinity and tritium distributions and their causes are examined. The results are discussed in section 5 and summarized in section 6.

## 2. Model

### *a. Model description*

The OGCM we use here is GFDL MOM 1.1 (Pacanowski et al. 1991). The model covers the portion of the Pacific from 50°S to 60°N and has realistic coastline and bottom topography with the maximum depth at 5000 m. The model solves the primitive equations on a spherical coordinate, under the Boussinesq, rigid lid, and hydrostatic approximations. The horizontal and ver-

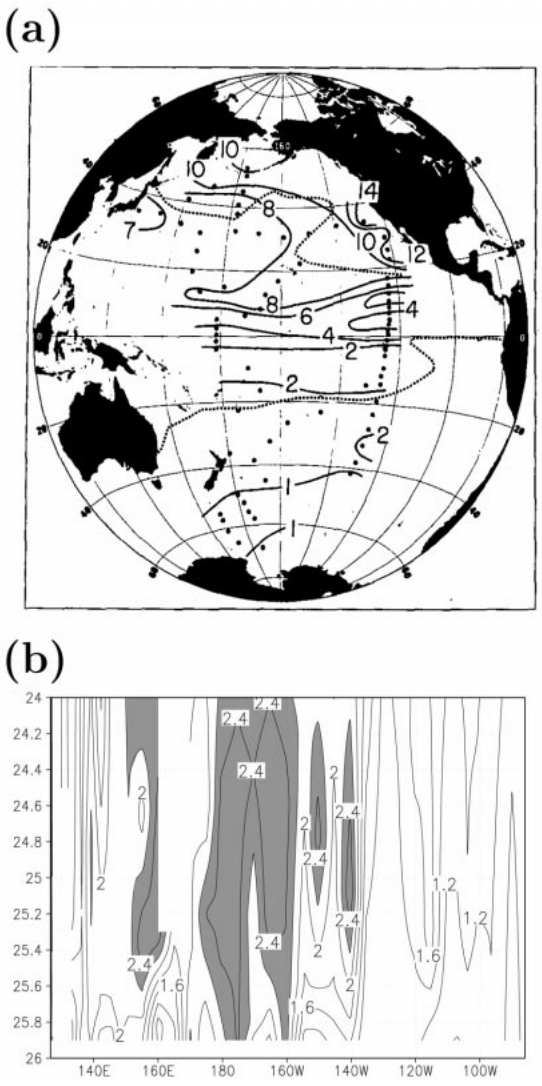


FIG. 3. (a) Tritium concentration (TU) on the $\sigma_\theta = 23.9$ surface. Tritium concentrations correspond to values on 1 Jan 1972 (after Fine et al. 1981). (b) Zonal vs $\sigma_\theta$ section of tritium concentration on WOCE P04 line along 10°N taken in early 1989. Contour intervals are 0.2 TU. Regions with TU $>$ 2.2 are shaded.

tical eddy viscosities are constant at $5.0 \times 10^7$ and 10.0 $cm^2\ s^{-1}$, respectively. Tracers are mixed both along isopycnal surfaces and diapycnally (Solomon 1971; Cox 1987) with diffusivities of $2.0 \times 10^7$ and 0.3 $cm^2\ s^{-1}$, respectively. Within 5 degrees of the model's poleward boundaries, temperature and salinity are restored to the prescribed climatological values with seasonal variation (Levitus and Boyer 1994; Levitus et al. 1994). The model employs a nonslip condition and requires the fluxes of mass, temperature, and salinity to vanish at all boundaries except at the sea surface where the climatological wind stress (Hellerman and Rosenstein 1983) is applied. Temperature and salinity are restored to the climatological value at the sea surface with a restoring time of 14 days for a water column of 10 m. Initially, the model ocean is at rest with the annual mean climatological temperature and salinity. The horizontal resolution is 1°, and there are 41 levels in the vertical with 10-m to 15-m resolutions in the top 300 m. The model is integrated for 31 years and is in a nearly steady state in the upper 500 m. The model result averaged for the last year is used in the following analyses. Our model reproduces quite well the current systems and the three-dimensional temperature distributions observed over the Pacific. Model output has been previously used to study the subduction of North Pacific interdecadal SST anomalies into the main thermocline (Nonaka et al. 2000).

### *b. The tropical salinity field in the OGCM*

The meridional section of the annual mean salinity of the model result in the central Pacific (155.5°W) shows the extensions of high salinity water in the upper thermocline in both hemispheres (Fig. 1b) as seen in the observed fields (Fig. 1a). Three tongues, the northern and southern high salinity tongues and the northern low salinity tongue, are found on the $\sigma_\theta = 24.5$ isopycnal surface (Fig. 2b). Although these tongues are more diffuse than those in the climatological fields (Fig. 2a), the large-scale salinity distributions in the tropical upper thermocline, on which we focus in this study, are well reproduced in our model. In the next section, we examine how these salinity distributions are formed in the model.

## 3. Forming of tropical salinity distribution

In Fig. 2b, trajectories of water parcels following the annual mean flow fields are superimposed upon the isopycnal salinity fields. High salinity tongues in both hemispheres extend in the direction of the currents deduced from the trajectories, consistent with the observed directions of the high and low salinity tongues and the geostrophic flow (Tsuchiya 1968). This shows that high salinity sea surface waters in the subtropics are subducted from the outcrop line into the thermocline and then advected by the ocean circulation to the Tropics, forming the high salinity tongues. Some trajectories return poleward after arriving at the western boundary, showing that part of the subducted high salinity water recirculates within the subtropics.

The low salinity tongue along about 10°N is formed by both low salinity water subducted from the eastern part of the North Pacific and water with salinity lowered by mixing. Water advected to the western boundary with low salinity, represented by the trajectory from 140°W (solid line in Fig. 4), originally has higher salinity. Its salinity is, however, lowered on the way to about 15°N (Fig. 4b) mainly by isopycnal mixing with eastern low salinity water (Figs. 4c,d). On the other hand, salinity of eastern low salinity water (short-dashed line in Fig. 4) continuously increases while traveling southward mainly by isopycnal mixing with western high-salinity

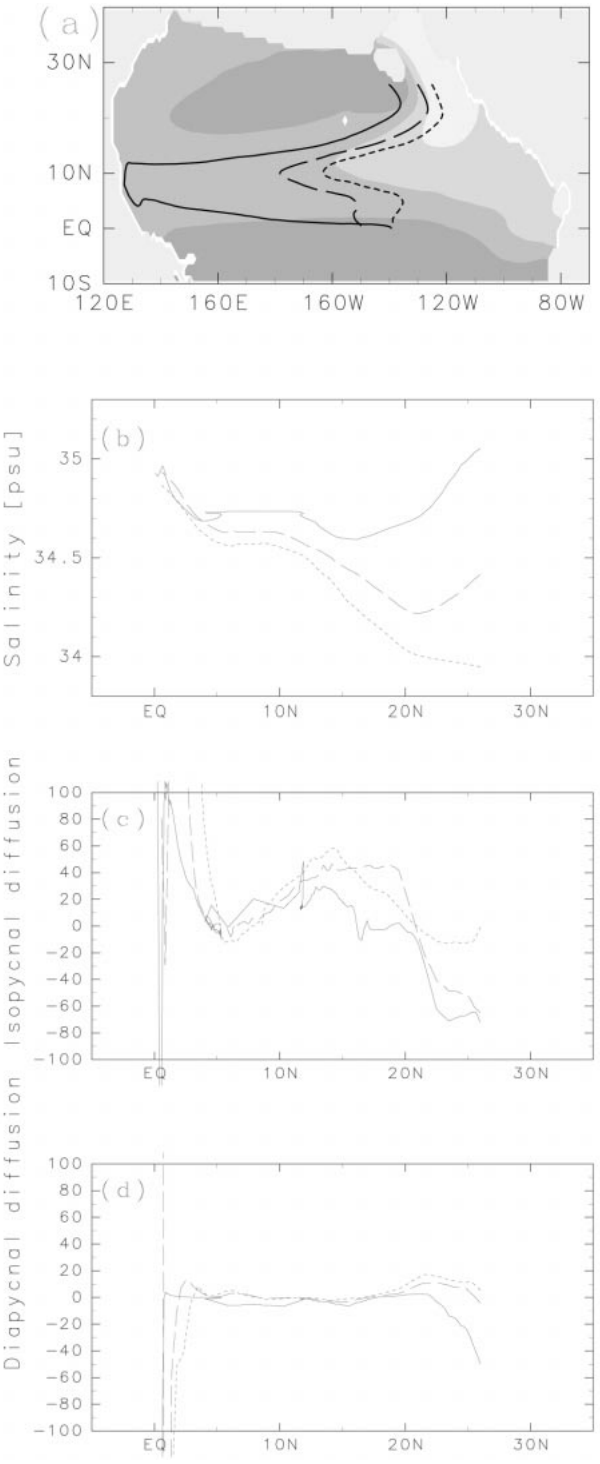


FIG. 4. (a) Salinity on the isopycnal surface $\sigma_\theta = 24.5$ (shaded) and trajectories of water parcels starting at 26°N, 140°W (solid), 130°W (long-dashed), and 125°W (dashed) on the same surface. Boundaries of shadings are at 34.2, 34.5, and 34.8 psu. Darker shading shows higher salinity. (b) Salinity on the trajectories shown in (a). Each line corresponds to the trajectory shown in the same line type. (c, d) Salinity budget balance on the same trajectories. (c) and (d) show, the isopycnal and diapycnal mixing ($\times 10^{-13}$ psu s$^{-1}$), respectively.

water. Salinity for the trajectory between these trajectories (long-dashed line in Fig. 4) decreases near 20°N by mixing with eastern low salinity water, and after that it increases by mixing with more saline western water. These eastern trajectories show that low salinity water subducted from the eastern part of the North Pacific extends southwestward only to the central Pacific (dashed lines in Fig. 4a), and thus the western part of the low salinity tongue extending onto the western boundary is formed by the water whose salinity is lowered by mixing (solid line in Fig. 4).

As shown by the trajectories (Fig. 2b), the southern high salinity water does not extend into the Northern Hemisphere beyond the equator, because water parcels approaching the equator are advected to the east by the Equatorial Undercurrent and then upwelled into the surface layer (Fig. 2c). Northern Hemisphere water does not extend into the Southern Hemisphere, either; thus, a front created by salinity differences forms between the Northern and Southern Hemisphere water at the equatorial region.

From the subtropical sea surface salinity (SSS) distributions in relation to the so-called exchange windows, the properties of the tropical salinity field in the upper thermocline are interpreted as follows. Here, the western boundary (interior) exchange window is defined as the region from which subducted water is transported to the equatorial region through the western boundary region (interior ocean) in the subsurface layer (Liu 1994; Nonaka 1998). In the Northern Hemisphere, high SSSs are found only in the western boundary exchange window (Fig. 5) and thus the northern high salinity tongue hits the western boundary before arriving at the equator. To the east of the high SSS region in the Northern Hemisphere, low SSSs are found in the interior exchange window (Fig. 5), and from there the low salinity tongue extends all the way to the equator through the interior ocean. In the Southern Hemisphere, on the other hand, high SSSs occupy both the interior and western boundary exchange windows, and thus the southern high salinity tongue extends to the equator through both the interior ocean and western boundary region (Fig. 2).

## 4. Discrepancy between salinity and tritium distributions

Like the hemispheric asymmetry of the salinity distribution mentioned above, the difference of the salinity and tritium distributions may be caused by the difference between the sea surface distributions of salinity and tritium relative to the exchange windows. As shown in Fig. 6a, the sea surface tritium field has high values off the coast of North America (Fine et al. 1981) within the interior exchange window (light shading in Fig. 6b). Thus, high tritium water subducted from near the eastern boundary would take the interior pathway to the equatorial region and form the high tritium tongue extending

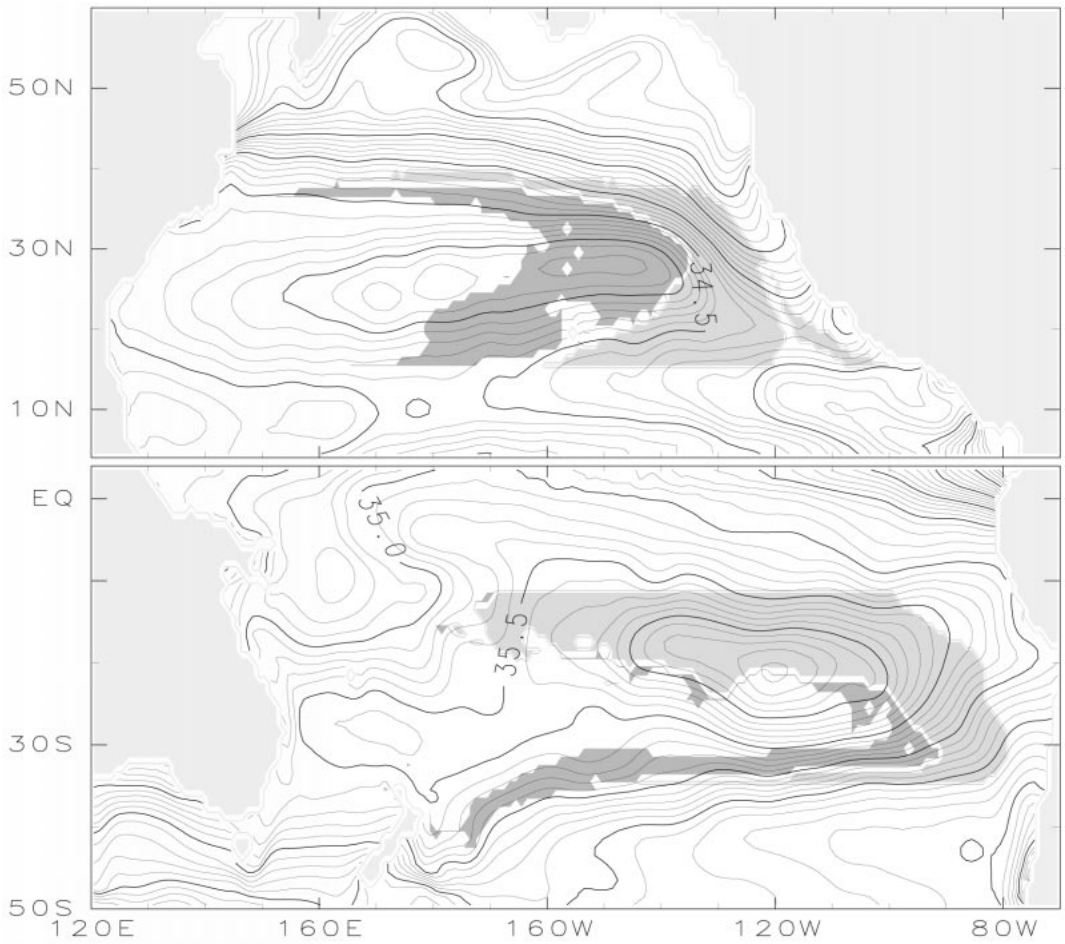


FIG. 5. Annual-mean sea surface salinity of the model result with the exchange windows. Contour intervals are 0.1 psu. The exchange windows are shaded. Dark (light) shade is the western boundary (interior) exchange window. To detect the exchange window, we follow the trajectories of water particles that start at all grid points from 15°N to 50°N and from 10°S to 50°S of 25 m depth with the annual-mean velocity field. The western boundary (interior) exchange window is defined as the group of the starting points of these trajectories that reach the equatorial region through the western boundary region (the interior ocean).

all the way to the equator through the interior ocean, as shown in Fig. 3.

To confirm this, we perform the tracer experiment as follows. A tracer that simulates tritium is injected into the model ocean by restoring tracer concentration to a prescribed distribution at the uppermost level. The restoring time is 14 days, the same as for salinity. The prescribed distribution (Fig. 6b) resembles the sea surface tritium field (Fig. 6a), which has maxima near the eastern boundary and has higher concentration in the higher latitude. This tracer is passive and does not affect the density and velocity fields. While continuously injecting this tracer from the sea surface, our model is integrated forward ten years from year 30.

On the meridional section at 180°, the tracer has its maximum value beneath the mixed layer between 5° and 20°N (Fig. 7a), similar to the observed tritium field (Fine et al. 1981, their Fig. 2a), although the modeled tracer concentration is not as high as the observed one. On the isopycnal surface, a high tracer concentration tongue extends from near the eastern boundary, where high tracer concentration is prescribed at the sea surface, southwestward all the way to the equatorial region through the interior ocean (Fig. 7b). The difference of salinity and tracer distributions in the upper thermocline is caused only by the difference of their sea surface distributions, because they are advected by the same flow field.

## 5. Discussion

It has been shown that isopycnal mixing is important in forming the low salinity tongue around 10°N (Fig. 4), which extends all the way to the western boundary. Therefore, formation of the low salinity tongue possibly depends on the larger isopycnal diffusion in the OGCM than in the real ocean, suggested by the more diffuse salinity tongues in the OGCM than in the climatology

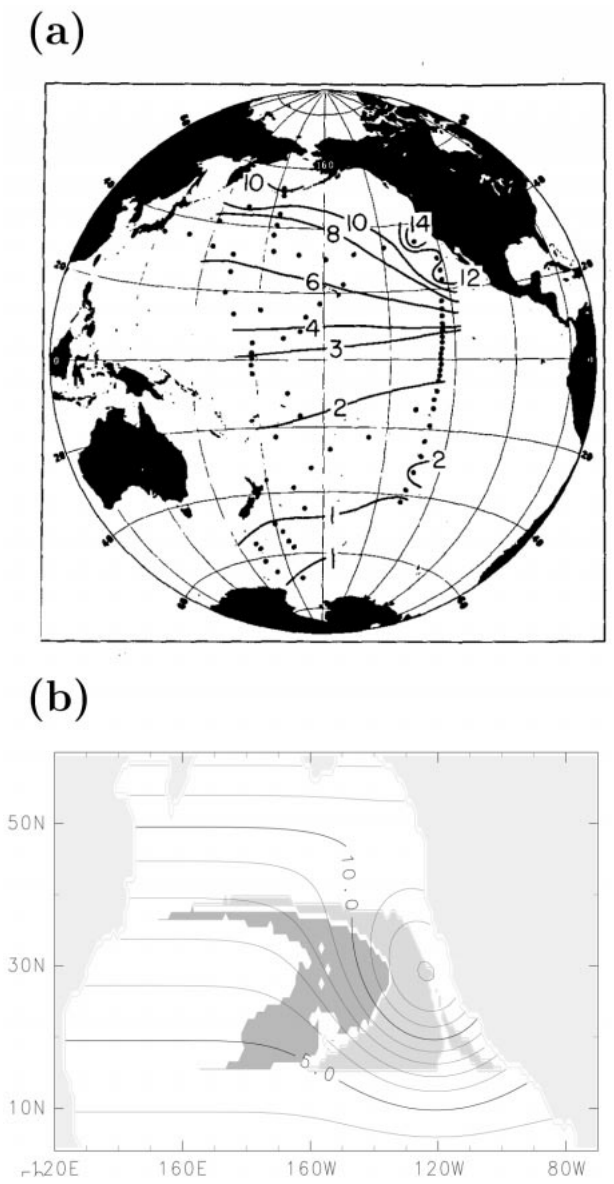


FIG. 6. (a) Tritium concentration at the sea surface at the time of the Pacific GEOSECS expedition, Aug 1973–Jun 1974 (after Fine et al. 1981). (b) Prescribed tracer concentration at the sea surface. Contour intervals are 1.0. Shades are same as Fig. 5. Tracer is injected to the model ocean by restoring tracer concentration in the uppermost level to this field.

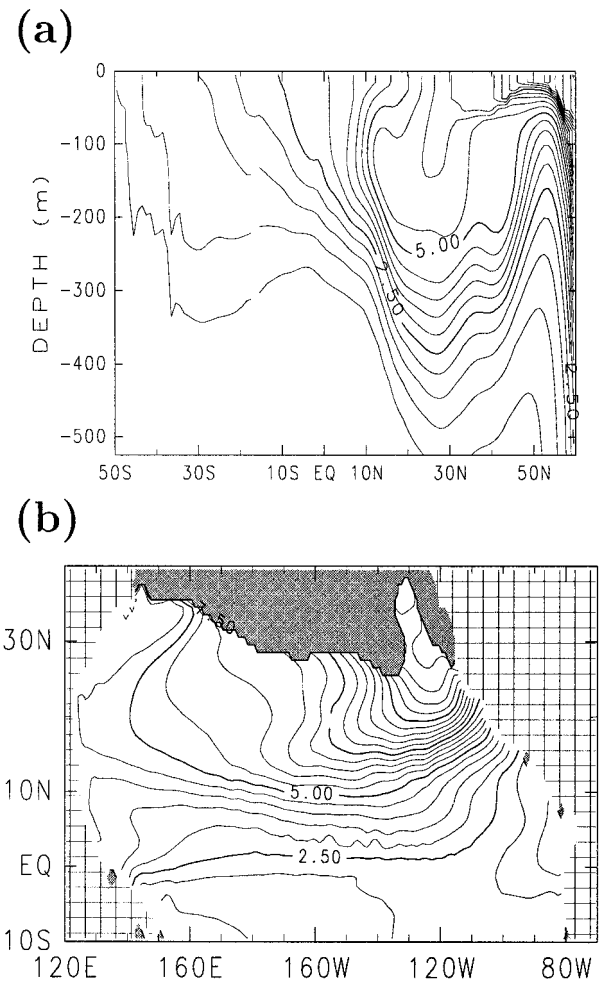


FIG. 7. Tracer concentration of the model result at year 10 of the passive tracer experiment, on (a) meridional section at 180° and (b) the $\sigma_\theta$ = 24.5 isopycnal surface. Dark shaded region shows outcropping area. Contour intervals are 0.5.

(Figs. 2a,b). To examine this dependency, we perform a sensitivity experiment with isopycnal diffusivity reduced by half, to $1.0 \times 10^7$ cm$^2$ s$^{-1}$. The salinity field in this experiment shows sharper high and low tongues and thus is more realistic than the standard case (not shown). This shows that formation of the low salinity tongue does not depend on the magnitude of the isopycnal mixing in the standard case. The reason for the sharper low salinity tongue is a reduction of the diffusion that normally increases salinity of the tongue during extension to the western boundary (Fig. 4), while mixing to reduce salinity in the source region of the tongue is also weakened.

Diapycnal mixing is also possibly large enough so that the water parcel can break the Sverdrup transport constraint to block the interior equatorward flow caused by the weak Ekman downwelling around 10°N. As a result, water parcels subducted in the eastern part of the North Pacific may take a more interior pathway to the equator than in the real ocean, and thus the interior exchange window in the OGCM possibly has a larger zonal width than in the real ocean. However, because the low SSS (Fig. 5) and high sea surface tritium (Fig. 6a) in the eastern North Pacific extend all the way to the coast of North America, even if the real interior exchange window has smaller zonal width than that shown here, it would supply low salinity water and high tritium water, and thus the result would not change significantly. If the real ocean had no interior exchange window in the North Pacific, the tracer field would

change significantly: the tracer field would not show the high concentration tongue extending equatorward through the interior ocean. That result is, however, inconsistent with the observed tritium distribution.

The absence of an Indonesian Throughflow in our model may also affect the model ocean circulation. However, water parcels that leave the Pacific via the Indonesian Throughflow take routes northwest of the western boundary pathway (Lu et al. 1998) and thus would not significantly affect water parcels in the interior pathway discussed here, which flow southeast of the western boundary pathway.

## 6. Summary

By examining the mechanisms forming salinity distribution in the tropical upper thermocline, we have shown the reasons for the hemispheric asymmetry of the salinity distribution and the differences of salinity and tritium distributions. Our results suggest that the asymmetry is caused by differences of the SSS distributions in the subtropics relative to the exchange windows between both hemispheres.

Reproduction of a realistic tropical salinity distribution with an interior pathway in the North Pacific shows that the northern high salinity tongue reaches the equator only through the western boundary region, compatible with the interior pathway from the North Pacific to the equator. It is the low salinity tongue that reveals this interior pathway. Therefore, the northern tropical salinity and tritium distributions are not contradictory. The high salinity and tritium tongues suggest different types of pathways, namely a western boundary pathway and an interior ocean pathway, respectively. This difference between the salinity and tritium distributions is mainly caused by the difference of their sea surface distributions relative to the exchange windows in the subtropics. These different distributions of salinity and tritium formed by the same flow field raise caution in interpreting ocean circulation with tracer distributions alone.

*Acknowledgments.* We thank S.-P. Xie for reading an earlier version of our manuscript and giving us invaluable comments. R. Lukas gave us useful comments. J. Loschnigg did careful English editing and gave us some comments. We thank W. J. Jenkins and others who participated in the WOCE P04 cruises for providing the tritium data. This study is supported by grants from Frontier Research System for Global Change and University of Tokyo's Center for Climate System Research. The figures were produced by GFD-DENNOU library and GrADS.

REFERENCES

Cox, M. D., 1987: Isopycnal diffusion in a *z*-coordinate ocean model. *Ocean Modelling* (unpublished manuscripts), **74,** 1–5.

Fine, R. A., J. L. Reid, and H. G. Ostlund, 1981: Circulation of tritium in the Pacific Ocean. *J. Phys. Oceanogr.,* **11,** 3–14.

——, W. H. Peterson, and H. G. Ostlund, 1987: The penetration of tritium into the tropical Pacific. *J. Phys. Oceanogr.,* **17,** 553–564.

Gu, D., and S. G. H. Philander, 1997: Interdecadal climate fluctuations that depend on exchanges between the tropics and extratropics. *Science,* **275,** 805–807.

Hellerman, S., and M. Rosenstein, 1983: Normal monthly wind stress over the world ocean with error estimates. *J. Phys. Oceanogr.,* **13,** 1093–1104.

Johnson, G. C., and M. J. McPhaden, 1999: Interior pycnocline flow from the subtropical to the equatorial Pacific Ocean. *J. Phys. Oceanogr.,* **29,** 3073–3089.

Levitus, S., and T. P. Boyer, 1994: *World Ocean Atlas 1994,* Vol. 4: *Temperature*. NOAA Atlas NESDIS 3, U.S. Dept. of Commerce, Washington, DC, 117 pp.

——, R. Burgett, and T. P. Boyer, 1994: *World Ocean Atlas 1994,* Vol. 3: *Salinity*. NOAA Atlas NESDIS 3, U.S. Dept. of Commerce, Washington, DC, 97 pp.

Liu, Z., 1994: A simple model of the mass exchange between the subtropical and tropical ocean. *J. Phys. Oceanogr.,* **24,** 1153–1165.

——, and B. Huang, 1998: Why is there a tritium maximum in the central equatorial Pacific thermocline? *J. Phys. Oceanogr.,* **28,** 1527–1533.

Lu, P., and J. P. McCreary, 1995: Influence of the ITCZ on the flow of the thermocline water from the subtropical to the equatorial Pacific Ocean. *J. Phys. Oceanogr.,* **25,** 3076–3088.

——, ——, and B. A. Klinger, 1998: Meridional circulation cells and the source waters of the Pacific Equatorial Undercurrent. *J. Phys. Oceanogr.,* **28,** 62–84.

McCreary, J. P., and P. Lu, 1994: Interaction between the subtropical and equatorial ocean circulations: The subtropical cell. *J. Phys. Oceanogr.,* **24,** 466–497.

Nonaka, M., 1994: A numerical study of the ocean circulation in the tropical Pacific (in Japanese). M.S. thesis, Dept. of Geophysics, Hokkaido University, Sapporo, Japan, 61 pp.

——, 1998: A numerical investigation of the effects of the subtropics on the Tropics through the ocean circulation. Ph.D. dissertation, Hokkaido University, Sapporo, Japan, 124 pp.

——, S.-P. Xie, and K. Takeuchi, 2000: Equatorward spreading of a passive tracer with application to North Pacific interdecadal temperature variations. *J. Oceanogr.,* **56,** 173–183.

Pacanowski, R. C., K. W. Dixon, and A. Rosati, 1991: The GFDL Modular Ocean Model User's Guide. GFDL Ocean Group Tech. Rep. No. 2.

Rothstein, L. M., R.-H. Zhang, A. J. Busalacchi, and D. Chen, 1998: A numerical simulation of the mean water pathways in the subtropical and tropical Pacific Ocean. *J. Phys. Oceanogr.,* **28,** 322–342.

Shuto, K., 1996: Interannual variations of water temperature and salinity along the 137°E meridian. *J. Oceanogr.,* **52,** 575–595.

Solomon, H., 1971: On the representation of isentropic mixing in an ocean circulation model. *J. Phys. Oceanogr.,* **1,** 233–234.

Tsuchiya, M., 1968: Upper waters of the intertropical Pacific Ocean. *Johns Hopkins Oceanogr. Stud.,* **4,** 50 pp.

Wyrtki, K., and B. Kilonsky, 1984: Mean water and current structure during the Hawaii-to-Tahiti shuttle experiment. *J. Phys. Oceanogr.,* **14,** 242–254.

Xie, S.-P., 1996: Westward propagation of latitudinal asymmetry in a coupled ocean–atmosphere model. *J. Atmos. Sci.,* **51,** 3236–3250.